

identified by absorption in aluminum long after the disappearance of any Cu^{62} that might have been initially produced during the bombardment through the reaction $\text{Ni}^{60}(\text{He}^3, p)\text{Cu}^{62}$. The reaction involved is therefore $\text{Ni}^{60}(\text{He}^3, n)\text{Zn}^{62}$ for the 8.4-hour activity, whereas for the 3.4-hour activity it is $\text{Ni}^{60}(\text{He}^3, d)\text{Cu}^{62}$ and/or $\text{Ni}^{60}(\text{He}^3, pn)\text{Cu}^{62}$.

From the initial values of the different activities shown in Fig. 3, for which the duration of bombardment was 1 hour, the saturation intensities were calculated. The relative cross sections for production of the above activities were computed after having taken into consideration the decay characteristics of the product nuclei and the efficiency of the measuring equipment for the various radiations emitted. The results are

$$\sigma_{58}(1.5 \text{ days}) : \sigma_{58}(24.5 \text{ min}) : \sigma_{62}(12.9 \text{ hr}) : \\ \sigma_{60}(8.4 \text{ hr}) : \sigma_{60}(3.4 \text{ hr}) = 1 : 1 : 10 : 25 : 12.$$

The error in the calculation may not exceed 15 percent

except in the case of $\sigma_{60}(8.4 \text{ hr})$ where the uncertainty may amount to 50 percent introduced in the process of extrapolating intensities in Fig. 3.

IV. DISCUSSION

The above results, preliminary in nature, show the many radioactivities that are produced through numerous He^3 reactions. Sometimes as in the case of C^{11} , the resulting activity is free from other disturbing activities produced by customary bombarding particles. Activities that are produced with difficulty by $(\alpha, 2n)$ reactions with high energy alpha-particles, are easily produced by (He^3, n) reactions, which reactions, in the present study, are found to be quite prolific.

Grateful acknowledgment is made for an Ohio State University Graduate School Fellowship granted to one of the authors (J.K.L.). Thanks are also due the U. S. Atomic Energy Commission for an AEC predoctoral fellowship given to another (T.W.D.).

Lifetimes of Metastable States of Noble Gases

A. V. PHELPS* AND J. P. MOLNAR
Bell Telephone Laboratories, Inc., Murray Hill, New Jersey
(Received December 10, 1952)

The lifetimes of the lower metastable states of helium, neon, and argon have been studied as a function of the pressure and temperature of the parent gas and the size of the container. The lifetimes were determined from measurements of the decay constant of the radiation absorbed by the metastable atoms. At low metastable concentrations the loss is by diffusion to the walls of the absorption cell and by collisions with neutral atoms within the volume of the cell. The data indicate that at 300°K and sufficiently high pressures, the volume destruction of the lower neon metastable is directly proportional to the pressure as expected for two-body collisions. The volume destruction of the lower neon metastables at 77°K and the helium triplet metastables at 300°K and 77°K is proportional to the square of the pressure as for three-body collisions. The volume loss of the lower argon metastables at 300°K contains both linear and quadratic pressure dependent terms.

INTRODUCTION

THE general principles of the behavior of the metastable atoms of helium, neon, and argon in their parent gases were established by the experiments of Meissner and others.¹ These investigators employed experimental arrangements in which the density of metastables in the afterglow of an interrupted discharge was measured by the optical absorption observed at appropriate wavelengths. Their results were interpreted on the assumption that the metastable atoms were lost by diffusion to the walls of the containing vessel and by excitation to a radiating state in collisions

with neutral atoms. The measured diffusion coefficients and excitation cross sections were reasonable except in the case of helium, for which the excitation cross section required to explain Ebbinghaus² results was impossibly large.

Our interest in this problem arose from investigations of the pulsed Townsend discharge by one of us (J.P.M.) in which metastable lifetimes and diffusion coefficients could be measured.³ An optical experiment similar to that of Meissner was set up with the hope that the destructive processes involving collisions with neutral atoms might be further clarified. The experiment was "modernized" by using a photomultiplier as a light detector in conjunction with electronic timing circuits.⁴

* Now at Westinghouse Research Laboratories, East Pittsburgh, Pennsylvania.

¹ K. W. Meissner and W. Graffunder, *Ann. Physik* **84**, 1009, (1927); see also summaries by F. M. Penning and N. deGroot *Handbuch der Physik* (Julius Springer, Berlin, 1933), Vol. 23, and A. C. G. Mitchell and M. K. Zemansky, *Resonance Radiation and Excited Atoms* (University Press, Cambridge, 1934).

² E. Ebbinghaus, *Ann. Physik* **7**, 267 (1930).

³ J. P. Molnar, *Phys. Rev.* **83**, 933 (1951).

⁴ A similar "modernized" experimental arrangement is described by F. A. Grant, *Can. J. Research A28*, 339 (1950), and *Phys. Rev.* **84**, 844 (1951).

This arrangement enabled us to make observations much more quickly and somewhat more accurately than was possible with the photographic techniques used by earlier workers. The investigations were extended to higher pressures and lower temperatures by one of the authors (A.V.P.) during the summer of 1950. Although circumstances have not permitted us to carry these studies to completion, it is felt that our results lead to a more accurate picture of the processes responsible for the destruction of the metastable atoms than was previously possible.

The results presented in this paper for helium and argon differ qualitatively from those found previously by showing that the dominant destruction process at high pressures is a collision between the metastable and two neutral atoms. The two-body destruction process found previously for neon at 300°K is confirmed but does not dominate at 77°K. In general, the values obtained for the destruction probability of metastables by collisions with neutral atoms were found to be considerably smaller than the values obtained by earlier workers.⁵

THEORY

We propose the following processes to explain the destruction of metastable atoms which results from collisions of metastables with neutral atoms and other metastable atoms:⁶

1. Diffusion and de-excitation on collision with the walls.
2. Two-body collisions with neutral atoms resulting in
 - (a) excitation to a nearby higher radiating state;⁷
 - (b) de-excitation to a lower state;
 - (c) formation of unstable diatomic molecules which may radiate before dissociation, i.e., collision induced radiative transitions.
3. Three-body collisions with two neutral atoms, presumably resulting in the formation of a stable excited molecule.
4. Collisions between pairs of metastable atoms resulting in the ionization of one of the atoms and de-excitation of the other.⁸

Theoretical estimates of the coefficients associated with the various metastable destruction processes are available only in the case of the diffusion of the helium metastables through helium.⁹ Accordingly, the separa-

⁵ See Mitchell and Zemansky (reference 1).

⁶ The loss of metastable atoms due to their natural decay does not appear to be a significant process under the conditions of our experiments.

⁷ If the resonance radiation from the radiating state is imprisoned for a sufficient length of time [see T. Holstein, Phys. Rev. 72, 1212 (1947) and Phys. Rev. 83, 1159 (1951)], the destruction of the metastables by process 2a will be reduced. Although theoretical estimates indicate that this effect may be appreciable at high pressures in neon, the experimental data are not sufficiently accurate or extensive to permit us to ascribe the observed deviations from Eq. (2) to this process.

⁸ Effects of metastable-metastable collisions, as well as independent measurements of diffusion coefficients and cross sections for ionization of impurities, are presented by M. A. Biondi, Phys. Rev. 82, 453 (1951) and Phys. Rev. 88, 660 (1952).

⁹ R. A. Buckingham and A. Dalgarno, Proc. Roy. Soc. (London) A213, 506 (1952).

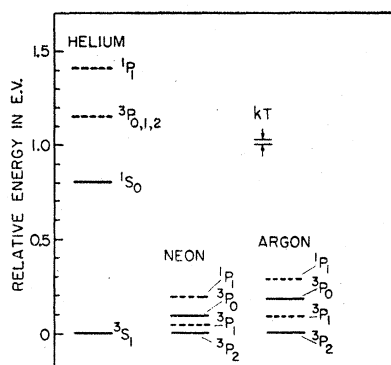


Fig. 1. Relative energy spacings of the states of the lowest excited electron configurations for three of the noble gas atoms. The radiating states are indicated by dashed lines, the metastable by solid lines. The electron configurations are $1s2s$ and $1s2p$ for helium, $2p^63s$ for neon, and $3p^64s$ for argon. In each case the lowest state, a metastable state, is taken as the zero of the energy scale. The electron-volt equivalent of kT for 300°K is also indicated.

tion of the various processes must be based on measurements of the time dependence of the decay of the metastable concentration and the pressure and temperature dependence of the associated decay constants. An estimate of the relative importance of process 2a for the various gases can be obtained from a consideration of the energy spacings of the metastable and nearby radiating states shown for helium, neon, and argon in Fig. 1. In each case the lowest excited state of the atom is metastable because the selection rules prevent electric dipole radiation to the $1S_0$ ground state. In the cases of neon and argon the lowest radiating state, $3P_1$, is located less than one-tenth of an electron volt above the lower metastable state, $3P_2$, so that process 2(a) is energetically possible in thermal collisions. For helium the lowest state which can radiate to the ground state is 1.4 electron volts above the metastable state. Thus, the destruction of helium triplet metastables by process 2(a), as assumed in the interpretation of Ebbinghaus^{11,2} data, seems virtually impossible at room temperatures. The upper metastable state, $3P_0$, in neon and argon can be destroyed by de-excitation to the lower radiating state, $3P_1$, as well as by excitation to the upper radiating state, $1P_1$.

The rate of change of the metastable concentration as a result of the processes listed above is

$$\partial M / \partial t = (D_0 / \bar{p}) \nabla^2 M - A \bar{p} M - B \bar{p}^2 M - \alpha M^2. \quad (1)$$

Here M is the metastable concentration, D_0 is the diffusion coefficient for the metastables at one mm of Hg, \bar{p} is the pressure in mm of Hg, A is the frequency of destruction by two-body collisions at one mm pressure [processes 2(a), 2(b), and 2(c)], B is the frequency of destruction by three-body collisions at one mm pressure, and α is the ionization frequency per unit metastable concentration.

The solution of Eq. (1) for the time dependence of the metastable concentration can be obtained in a

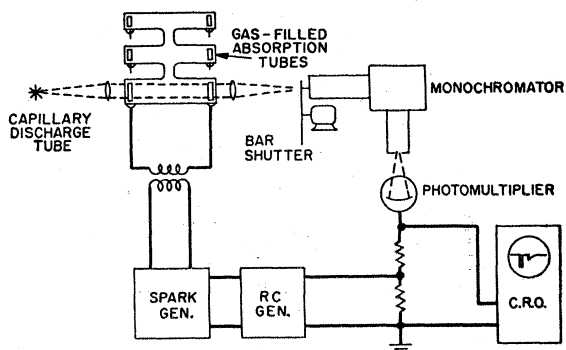


FIG. 2. Schematic diagram of the apparatus used in the metastable decay studies. The Gaertner monochromator had glass lenses and a heavy flint glass prism for high dispersion in the red and infrared.

closed form only in the limits of low and high metastable densities. At low metastable densities the last term of Eq. (1) can be neglected. If we restrict our solution to times sufficiently late in the afterglow, only the lowest diffusion mode will be significant and the metastable density will decay exponentially with time. The decay constant is

$$1/\tau = D_0/(\rho\Lambda^2) + A\rho + B\rho^2, \quad (2)$$

where Λ is the diffusion length of the container and for a cylindrical vessel of radius R , and length L is given by $\Lambda = [(\pi/L)^2 + (2.4/R)^2]^{-1/2}$. The parameters D_0 , A , and B can be evaluated from measurements of $1/\tau$ as a function of the pressure and the size of the absorption cell. Further details concerning the individual processes can be obtained from studies of the variation of the parameters, D_0 , A , B , and α with the gas temperature.

At high metastable densities the destruction of metastables in collisions between pairs of metastable atoms will be large compared to the loss due to diffusion and collisions with neutral particles. The solution of Eq. (1) is then

$$1/M = 1/M_0 + \alpha t, \quad (3)$$

where M_0 is the metastable concentration at the beginning of the afterglow. Thus, if the plot of $1/M$ as a function of time is a straight line over a reasonable range of metastable densities, we can evaluate α and the cross section for collisions between pairs of metastable atoms.

EXPERIMENTAL ARRANGEMENT

A schematic diagram of the experimental apparatus used in these investigations is shown in Fig. 2. The gas to be studied is contained in a cylindrical absorption cell with flat windows and ring electrodes and is broken down periodically (15 to 60 cps) with a pulse from a spark generator lasting approximately 100 microseconds. The line spectrum of the gas being studied is obtained from a hot-cathode discharge tube. The section of the positive column used as the source of radiation

is confined by a capillary 0.5 mm in diameter. The radiation which has traversed the absorption cell is passed through a monochromator and detected with a photomultiplier. The output of the photomultiplier is developed across a resistance network and observed with an oscilloscope. The upper oscillograph trace of Fig. 3 shows the output of the photomultiplier under nearly ideal conditions. The downward spike at the left is produced by the interruption of the light by the bar shutter shown in Fig. 2 and indicates 100 percent absorption. This is followed by the sharp rise and slow decay of the absorption due to the metastables produced during the very short discharge pulse.

A simple means for measuring the decay constant of the absorption is provided by using the spark generator to trigger the discharge of a condenser and passing the subsequent current through the resistance network in order to subtract an exponentially varying signal from the output of the photomultiplier. The operation of this exponential comparison circuit is illustrated by the oscilloscope traces shown in Fig. 3. When the exponential signal is adjusted for optimum cancellation of the photomultiplier trace, the lifetime of the metastable atoms can be obtained from the RC time constant of the exponential signal.

The absorption cells were filled from a vacuum system designed to give minimum contamination of the

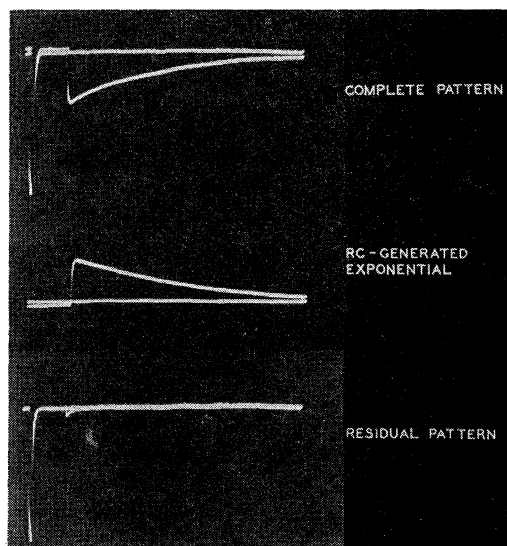


Fig. 3. Oscilloscope traces illustrating the operation of the time constant measuring circuit. The upper trace shows the photomultiplier output. The vertical spike at the left side represents the complete interruption of the light by the bar shutter shown in Fig. 2, and its lowest extension indicates the level of 100 percent absorption. For each trace the repetition rate of the horizontal sweep was set at 30 cps, whereas the sparking rate was set at 15 cps; thus the pattern is initiated by the spark in one sweep and continues through the second. The second trace shows the electronically generated exponential curve. The last trace shows the first two combined, with the second one adjusted in amplitude and time constant for optimum match. The example shown here illustrates operation under conditions of exceptionally low noise.

gas samples. The oil manometer and the stopcocks were separated from the absorption cell by two liquid nitrogen traps. The absorption cells and one trap were baked at 450°C overnight and the electrodes outgassed by induction heating. The gas was obtained from flasks of Airco reagent grade gas and passed over a freshly prepared barium surface. The absorption cells varied in size from six feet long and six inches in diameter to two inches long and 0.4 inch in diameter. The data at 77°K were obtained with a cell that was three feet long and three inches in diameter. It was equipped with a full-length liquid nitrogen-filled jacket. Evacuated end windows were provided to reduce frosting.

A number of precautions were taken to insure reliability in the measurements. The intensity of the light beam used for the absorption measurements in argon and neon was maintained at a level low enough to prevent appreciable destruction of metastables by exciting them to higher levels from which alternate radiative decay paths to the ground state are available. (In helium the 3S_1 metastable is immune to such light destruction.) The absorption curves were fitted to the electronically generated exponential curve in the region of 20 percent or less absorption, since only in this region can one assume that the observed absorption is linearly proportional to the density of absorbing atoms.⁵

INTERPRETATION OF ABSORPTION CURVES

Typical absorption curves obtained for the metastable states and the lower radiating state of neon and argon are shown in Figs. 4 and 5. The absorption by the upper radiating state, 1P_1 , was very small and is not

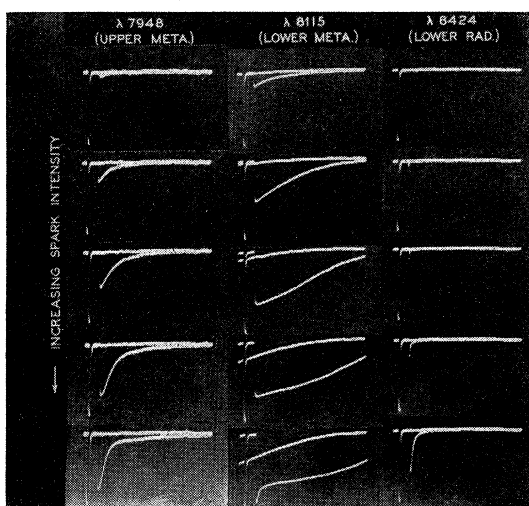


FIG. 4. Absorption curves illustrating the effect of increasing spark intensity for the 3P states of the $3p^4s$ configuration in argon ($p=1.0$ mm). The left column shows that the decay of the upper metastable (3P_0) density is not simply exponential. At the highest spark intensity a tail develops suggesting a decay rate comparable to that of the lower metastable state (3P_2) shown in the second column. The decay rate of the lower radiating state (3P_1) is very rapid at all spark intensities.

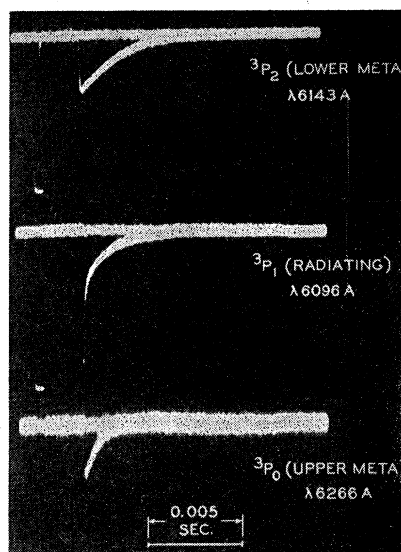


FIG. 5. Absorption traces for the 3P states in the $2p^63s$ configuration of neon ($p=7.5$ mm). The low noise level present in the neon experiments permits careful examination of the 3P_1 decay curve. The second trace shows the 100 percent absorption point produced by the bar shutter, a sharply decaying absorption starting from the 80 percent point, and a more slowly decaying part. The spark intensity was adjusted in each case to give roughly the same amplitude in the absorption curve, e.g., a maximum intensity for the 3P_1 case and a minimum intensity for the 3P_2 .

shown. As illustrated for argon by the curves of Fig. 4, the absorption curves for the 3P_0 and 3P_1 states in neon and in argon and the 1S_0 metastable state in helium either decayed too rapidly for accurate measurements or exhibited a form that varied greatly with spark intensity. We interpret the observed changes in the destruction rate with spark intensity at a given metastable density as indicating destruction of metastables by components other than neutral atoms and metastables, i.e., electrons or positive ions. The decay rates for the helium triplet metastable and the lower metastable states, 3P_2 , of neon and argon were found to be independent of the spark intensity except at the highest intensities. Therefore, the quantitative data presented in the following section refer only to the lower metastable states of the various gases.

The absorption curves of Fig. 5 provide qualitative evidence which supports the existence of processes 2(a) and 2(b) discussed under theory. The density of atoms in the lower radiating state, 3P_1 , can be seen to drop sharply after the termination of the spark and then to decay more slowly. Presumably the rapid initial decay corresponds to loss of these excited atoms by radiation, while the slow decay corresponds to a repopulation of the 3P_1 state as a result of de-excitation from the 3P_0 state or excitation from the 3P_2 state.

Most of our measurements were made in a range of pressure and discharge current such that the light beam traversed mainly the positive column of the dis-

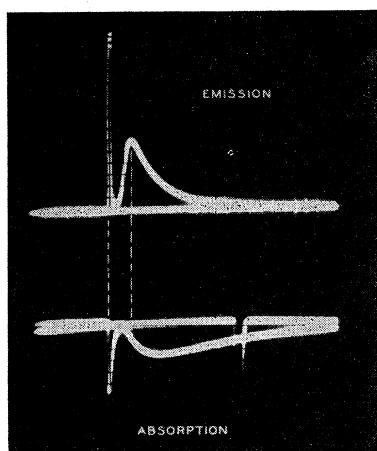


FIG. 6. Emission and absorption curves in the Faraday dark space region of a spark discharge in argon ($p=0.2$ mm). The absorption curve is for the 3P_2 state (8115A), while the emission curve represents the integrated light in the red region of the spectrum.

charge set up between the ring electrodes by the original spark. A specially built tube filled with argon at 0.2 mm of Hg was used to examine the absorption curves in various regions of the discharge. The initial metastable destruction rate was especially large in the regions near the cathode and in the striations of the positive column. The absorption curve for the Faraday dark space is shown in Fig. 6. The original metastable density falls almost to zero shortly after the termination of the spark, then builds up, and finally decays with a time constant approximately equal to that found in the

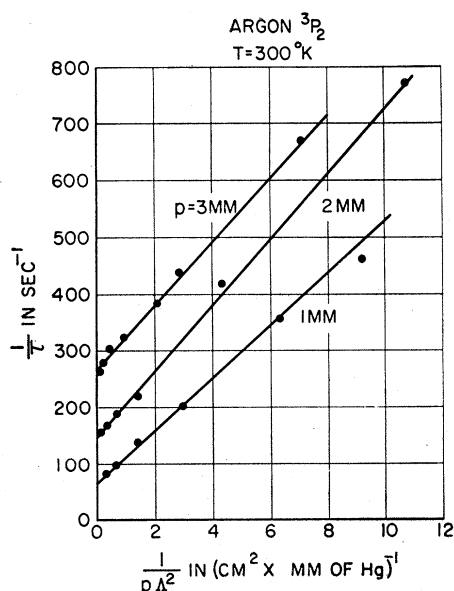


FIG. 7. Data taken with argon ($T=300^\circ\text{K}$) illustrating the method for separating the contributions of diffusion loss and volume loss to the measured decay constant, $1/\tau$, by varying the diffusion length Λ . The data were obtained using a set of interconnected absorption cells such as illustrated in Fig. 2.

positive column. The light generated in this region is shown by the upper curve of Fig. 6 and has the characteristic form of an afterglow. We explain these observations by assuming that fast electrons are present in the discharge after the spark is terminated, and that these destroy the metastables by excitation or ionization. As the electrons lose their initial kinetic energy they recombine with positive ions to produce atoms in the excited states and in the ground state. Radiative decay of the highly excited atoms produces the emitted light as well as metastables so that the maximum emission occurs at the same time as the maximum rate of increase of the metastable density.

RESULTS

Most of the quantitative data reported in this paper were obtained at low metastable densities where the absorption appeared to decay exponentially with time. Accordingly, we will analyze the data in terms of the expression for the decay constant, $1/\tau$, given by Eq. (2).

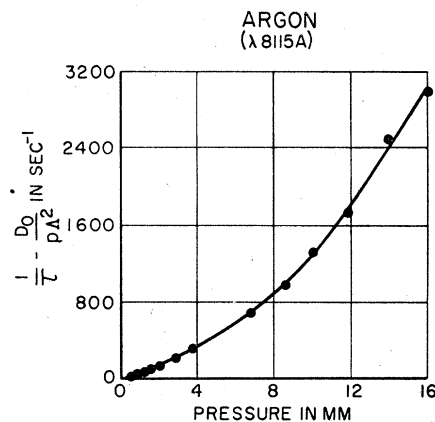


FIG. 8. Volume loss in argon as a function of pressure for the 3P_2 state (8115A) for 300°K and $\Lambda^2=2.4$ cm².

Figure 7 shows the results of measurements of the lifetimes of the lower argon metastable (using $\lambda 8115\text{A}$) as a function of the size of the absorption cell at various pressures. Equation (2) shows that the slope of the plot of the $1/\tau$ as a function of $1/(p\Lambda^2)$ gives the diffusion coefficient for the metastables at one mm pressure. The average diffusion coefficient at 300°K is 54 cm² sec⁻¹ compared to 45 cm² sec⁻¹ obtained from measurements of the transient build-up of a Townsend discharge.³ The loss of metastables as a result of collisions with neutral gas atoms can be found by subtracting the loss by diffusion from the measured destruction frequencies. Figure 8 shows the results of such a calculation for the lower argon metastable at 300°K . The smooth curve is the result of fitting the sum of a linear and a quadratic term to the experimental data, i.e., $A=40$ sec⁻¹ mm⁻¹ and $B=9$ sec⁻¹ mm⁻² in Eq. (2). Thus it appears that at 300°K the lower argon metastables are destroyed by both two- and three-body collisions. The data obtained at 77°K were not sufficiently reproducible to be con-

sidered in detail, but suggested a slow variation in the three-body destruction with temperature.

Figure 9 shows the results of a set of time constant measurements obtained from the absorption of the 6143A line by the lower neon metastable. The data at 77°K have been normalized with respect to changes in gas density by multiplying the pressure readings by 300/77. The smooth curves represent a fit of Eq. (2) to the experimental data with $A = 50 \text{ sec}^{-1} \text{ mm}^{-1}$, $B = 0$ at 300°K; and $A = 0$, $B = 5 \times 10^{-2} \text{ sec}^{-1} \text{ mm}^{-2}$ at 77°K. Thus, the loss of the lower neon metastable at 300°K appears to be by diffusion at the lower pressures and by either excitation to a radiating state [process 2(a)] or collision-induced radiation [process 2(c)] at the higher pressures. The measured destruction probability at 77°K shows that within the experimental error the loss of the 3P_2 metastables is by diffusion and by destruction in three-body collisions. The average diffusion coefficients at 300°K and 77°K were 150 cm^2/sec and 60 cm^2/sec at a density corresponding to one mm pressure

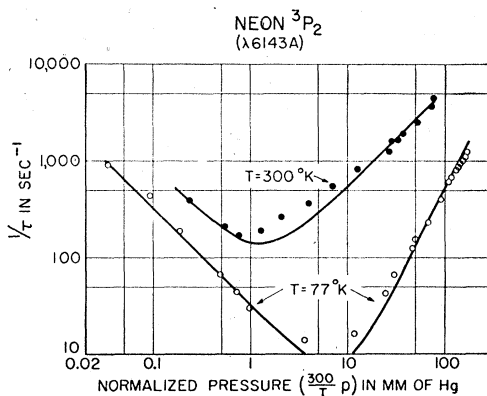


FIG. 9. Data showing $1/\tau$ as a function of normalized pressure in neon for the 3P_2 states (6143A) at 77°K and 300°K and for $\Lambda^2 = 1.9 \text{ cm}^2$.

at 300°K. The absence of an approximately linear pressure dependent term in the volume destruction at 77°K requires that the frequency of the process decrease by a factor of at least 200 as the temperature is reduced from 300°K to 77°K. This corresponds to an "activation" energy for the two-body destruction process which is at least as large as the spectroscopic energy difference between the 3P_2 and 3P_1 states. It should be noted that the decay constants obtained using the $\lambda 6402\text{A}$ line were approximately 20 percent lower than the values given in Fig. 9. The departure of the measured decay constants from the analytical curve at intermediate pressures is reproducible⁴ but is as yet unexplained.

Figure 10 is a summary of the decay constant measurements for the helium triplet metastable made using the 10 830A line. The plots of the measured values of $1/\tau$ as a function of normalized pressure, though scattered, are consistent with the interpretation that the loss of metastables is characteristic of diffusion at the

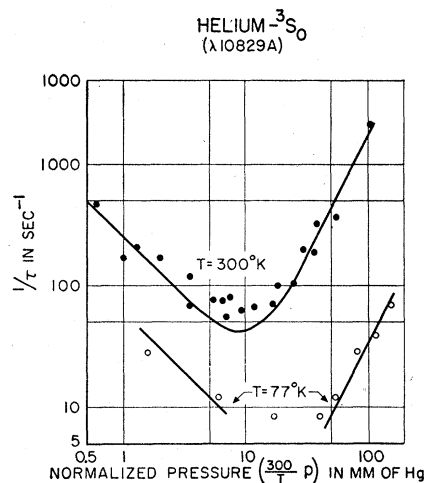


FIG. 10. Data showing $1/\tau$ as a function of normalized pressure in helium for the 3S_1 state (10 830A) at 77°K and 300°K for $\Lambda^2 = 1.9 \text{ cm}^2$.

lower pressures and is proportional to the square of the pressure at the higher pressures. The smooth curves were obtained by fitting Eq. (2) to the observed data with $A = 0$. The average diffusion coefficient for 300°K and one mm Hg is 410 cm^2/sec while that for 77°K and one mm Hg is approximately 130 cm^2/sec , showing a somewhat larger variation with temperature than that observed for neon. These values agree satisfactorily with the theoretical values of 370 and 130 cm^2/cm obtained by Buckingham and Dalgarno.⁹ The diffusion measurements showed that the loss varied as $1/\Lambda^2$ for Λ^2 between 0.04 cm^2 and 6.3 cm^2 within the experimental error of approximately 20 percent. The decrease in the volume loss from $0.2p^2 \text{ sec}^{-1}$ to $3 \times 10^{-3}p^2 \text{ sec}^{-1}$ as the temperature was changed from 300°K to 77°K suggests that the three-body collision process responsible for the destruction of the metastables has

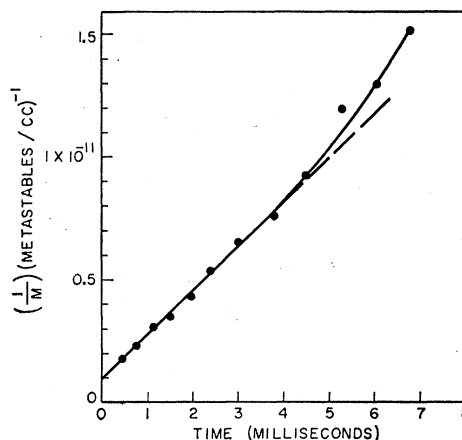


FIG. 11. Plot showing the reciprocal of the metastable density as a function of time. The data were obtained from an analysis of a photograph of the absorption of the 3889A line by helium triplet metastables at 300°K and 10 mm of Hg pressure.

TABLE I. Average cross section for the destruction of metastables of rare gas atoms by various impurities.

Metastable	Impurity	Average cross section, cm ²
A (³ P ₂)	Hg	3×10 ⁻¹⁶
A (³ P ₂)	Kr	1×10 ⁻¹⁶
A (³ P ₂)	H ₂	3×10 ⁻¹⁷
Ne (³ P ₂)	A	2×10 ⁻¹⁶
He (³ S ₁)	A	3×10 ⁻¹⁷

an activation energy of the order of 0.03 electron volt. The presence of an activation energy is consistent with the long range repulsive interaction calculated for the helium metastable and a normal helium atom.⁹

The volume loss for the helium triplet metastable obtained from this experiment is less than $\frac{1}{10}$ of that calculated by Ebbinghaus when his rather limited measurements were interpreted in terms of destruction by excitation to the nearest radiating state. The large volume loss of triplet metastables found by Ebbinghaus may well have been due to collisions between pairs of metastable atoms. We were able to estimate the cross section for destructive collisions between pairs of metastable atoms by analyzing a photograph of the absorption curve obtained at high metastable densities where the last term of Eq. (1) dominates the metastable destruction. Thus, Fig. 11 shows that when the nonlinear absorption of the 3889A radiation is taken into account,¹⁰ the reciprocal of the metastable density is a linear function of time over an appreciable range of metastable densities as predicted by Eq. (3). Using the theoretical absorption coefficient¹¹ to calculate the absolute metastable density, the average cross section for collisions between pairs of helium triplet metastable atoms is found to be 10⁻¹⁴ cm² at 300°K. We can now estimate the error in the time constant determinations due to collisions between pairs of metastable atoms. For the measurements summarized in Fig. 10, ten percent absorption corresponds to an average metastable density of 1.5×10¹⁰ metastable/cc. Therefore, the loss due to collisions between pairs of metastables amounts to about 20 percent of the measured loss at intermediate pressures and 300°K, but becomes negligible at the lower and higher pressures.

¹⁰ A correction for nonlinear absorption was made using the relations developed by Mitchell and Zemansky for Doppler broadening (see reference 1). The effective ratio of the line widths was determined by noting the change in absorption when the absorption path length was doubled. The tables of fractional absorption as a function of the product of the absorption coefficient and the path length have been recomputed and extended for us by R. W. Hamming.

¹¹ D. R. Bates and A. Damgard, *Trans. Roy. Soc. (London)* **A242**, 101 (1949).

Destruction of Metastables by Impurities

In order to estimate the effects of foreign gas impurities on the lifetimes of metastable atoms, small amounts of nitrogen, hydrogen, mercury, krypton, and argon were admitted to the absorption cells. Except in the cases of krypton in argon and argon in neon and helium, the foreign gas impurity was "cleaned up" by the discharge and the uncertainty in the admixture fraction is large. Table I gives the average results expressed in terms of the cross section for the destruction of metastables by the impurity atoms at 300°K. The cross sections for argon in helium and neon are in reasonable agreement with those obtained by Biondi from ionization studies.⁸ It should be noted that Biondi's measurements of ionization in helium may refer to the helium singlet metastable whereas our data certainly apply to the triplet metastable.

SUMMARY

Our measurements of the lifetimes of metastable atoms at low metastable densities have shown that the destruction of the metastables is by diffusion to the walls at low pressures and by either two-body or three-body collisions at high pressures. These experiments have demonstrated for the first time the importance of three-body collisions as a destruction mechanism for the lower metastable states of argon, neon, and helium. The fact that the observed decay constants for the helium triplet metastable yield reasonable coefficients for the rates of diffusion, three-body collisions, and collisions between pairs of metastables should remove the doubts which have been expressed⁵ regarding the validity of the absorption method. In particular, the agreement between the experimental and theoretical diffusion coefficients for the helium triplet metastable should serve to encourage further theoretical and experimental work in this field.

These studies have shown that there are many features of the destruction of the metastables which we could explain only qualitatively. A program directed toward correlated measurements of electron densities and more precise determinations of the metastable densities is being undertaken by one of us (A.V.P.).

The authors wish to express their appreciation to R. G. Brandes, H. C. Geissler, and H. W. Weinhart for their assistance in design and operation of the apparatus, and to P. W. Anderson, J. A. Hornbeck, and A. H. White for many valuable discussions. One of us (A.V.P.) wishes to thank the staff of the Bell Telephone Laboratories for the opportunity to participate in this research during the summer of 1950.

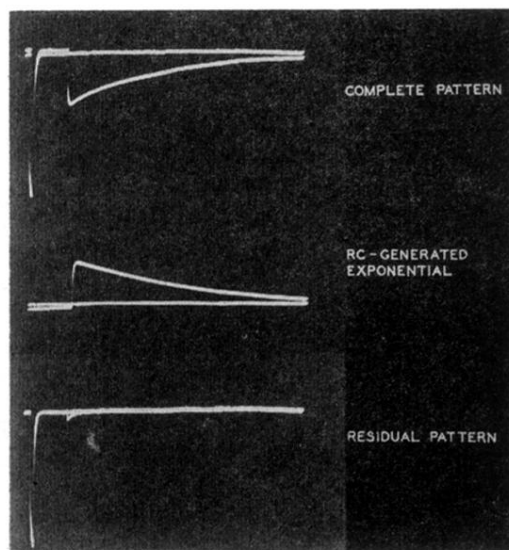


Fig. 3. Oscilloscope traces illustrating the operation of the time constant measuring circuit. The upper trace shows the photo-multiplier output. The vertical spike at the left side represents the complete interruption of the light by the bar shutter shown in Fig. 2, and its lowest extension indicates the level of 100 percent absorption. For each trace the repetition rate of the horizontal sweep was set at 30 cps, whereas the sparking rate was set at 15 cps; thus the pattern is initiated by the spark in one sweep and continues through the second. The second trace shows the electronically generated exponential curve. The last trace shows the first two combined, with the second one adjusted in amplitude and time constant for optimum match. The example shown here illustrates operation under conditions of exceptionally low noise.

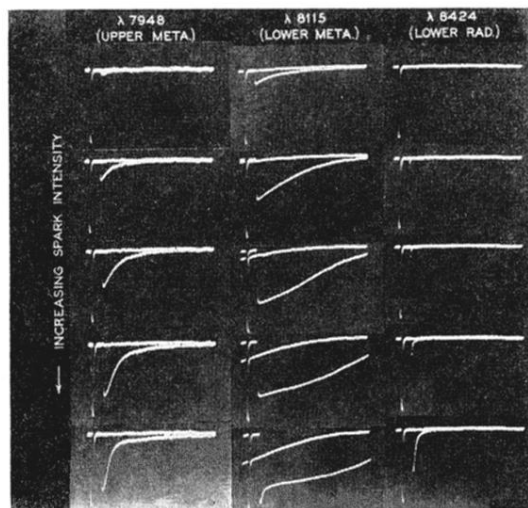


FIG. 4. Absorption curves illustrating the effect of increasing spark intensity for the 3P states of the $3p^5 4s$ configuration in argon ($p=1.0$ mm). The left column shows that the decay of the upper metastable (3P_0) density is not simply exponential. At the highest spark intensity a tail develops suggesting a decay rate comparable to that of the lower metastable state (3P_2) shown in the second column. The decay rate of the lower radiating state (3P_1) is very rapid at all spark intensities.

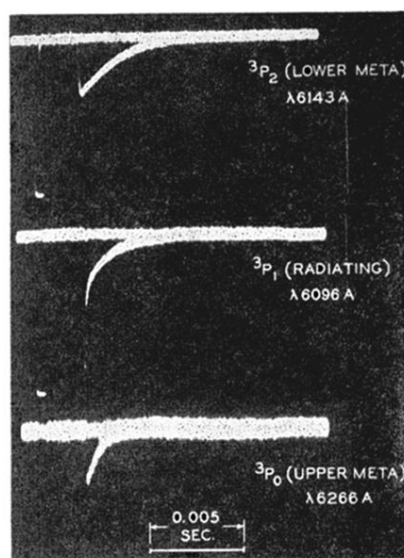


FIG. 5. Absorption traces for the 3P states in the $2p^43s$ configuration of neon ($p=7.5$ mm). The low noise level present in the neon experiments permits careful examination of the 3P_1 decay curve. The second trace shows the 100 percent absorption point produced by the bar shutter, a sharply decaying absorption starting from the 80 percent point, and a more slowly decaying part. The spark intensity was adjusted in each case to give roughly the same amplitude in the absorption curve, e.g., a maximum intensity for the 3P_1 case and a minimum intensity for the 3P_2 .

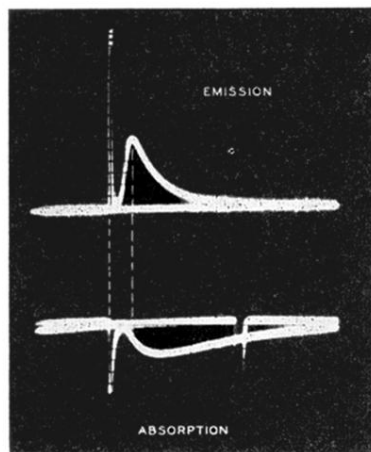


FIG. 6. Emission and absorption curves in the Faraday dark space region of a spark discharge in argon ($p=0.2$ mm). The absorption curve is for the 3P_2 state (8115Å), while the emission curve represents the integrated light in the red region of the spectrum.